Dossier

This paper is a part of the hereunder thematic dossier published in OGST Journal, Vol. 69, No. 5, pp. 773-969 and available online here

Cet article fait partie du dossier thématique ci-dessous publié dans la revue OGST, Vol. 69, n°5, pp. 773-969 et téléchargeable ici

DOSSIER Edited by/Sous la direction de : **P.-L. Carrette**

PART 1
Post Combustion CO_2 Capture
Captage de CO_2 en postcombustion

Oil & Gas Science and Technology – Rev. IFP Energies nouvelles, Vol. 69 (2014), No. 5, pp. 773-969

Oil & Gas Science and Technology – Rev. IFP Energies nouvelles, Vol. 69 (2014), No. 5, pp. 903-914

DOI: 10.2516/ogst/2012089

Dossier

Post Combustion CO_2 Capture
Captage de CO_2 en postcombustion

Piperazine/N-methylpiperazine/ N,N'-dimethylpiperazine as an Aqueous Solvent for Carbon Dioxide Capture

Stephanie A. Freeman, Xi Chen, Thu Nguyen, Humera Rafique, Qing Xu and Gary T. Rochelle*

Department of Chemical Engineering, The University of Texas at Austin, 1 University Station C0400, Austin, TX 78712 - USA
e-mail: sfreeman@che.utexas.edu - xi.a.chen@power.alstom.com - tnguyen02_2000@yahoo.com - hrafique@bechtel.com
qing.xu06@gmail.com - gtr@che.utexas.edu

* Corresponding author

Résumé — **Mélange pipérazine/N-méthylpipérazine/N,N'-diméthylpipérazine en solution aqueuse pour le captage du CO_2** — Un mélange pipérazine (PZ), N-méthylpipérazine (MPZ) et N,N'-diméthylpipérazine (DMPZ) en solution aqueuse est décrit pour le captage du CO_2 par absorption-régénération. Par rapport à la pipérazine concentrée, ce mélange permet un gain sur la solubilité des produits solides et sur la chaleur d'absorption. Aucune insolubilité n'a été observée à fort taux de charge en CO_2 contrairement aux solvants à base de pipérazine. Ce mélange a montré des performances équivalentes à la pipérazine concentrée en termes de capacité et de cinétique d'absorption du CO_2, qui sont plus que doublées par rapport à la traditionnelle MonoEthanolAmine (MEA) à 7 M (30 % massique). Un équilibre s'est établi entre les trois constituants qui augmente la stabilité thermique en comparaison des mélanges traditionnels de solvants. Le principal inconvénient de ce nouveau système est une volatilité plus importante des amines dans les conditions de l'absorbeur en comparaison avec le cas de la pipérazine concentrée et de la MEA.

Abstract — ***Piperazine/N-methylpiperazine/N,N'-dimethylpiperazine as an Aqueous Solvent for Carbon Dioxide Capture*** — *A blend of piperazine (PZ), N-methylpiperazine (MPZ) and N,N'-dimethylpiperazine (DMPZ) is described as a novel CO_2 capture solvent for aqueous absorption-stripping. This blend provides improved solid solubility and heat of absorption compared to concentrated PZ. No insolubility was observed for regions of high CO_2 loading, unlike PZ solvents. The blend performed like concentrated PZ in terms of CO_2 capacity and CO_2 absorption rate, both of which were more than double that of a traditional 7 molal (30 wt%) MonoEthanolAmine (MEA). Thermal equilibrium was established between the three constituent amines that increases the thermal stability compared to traditional blended solvents. The primary drawback of this novel solvent system is enhanced amine volatility at absorber conditions compared with both concentrated PZ and MEA.*

INTRODUCTION

Amine-based absorption-stripping is the most promising solution for post-combustion carbon dioxide (CO_2) capture from coal-fired power plant flue gas. Advanced amine solvents such as concentrated, aqueous piperazine (PZ) are being proposed to replace traditional alkanolamines such as MonoEthanolAmine (MEA) due to advantageous CO_2 absorption rates and overall energy performance [1, 2]. A new solvent concept proposed here is the use of amines that demonstrate noticeable levels of overall thermal degradation but degrade to useful products that can react with CO_2 and maintain alkalinity of the solution. One example of this solvent concept presented here is the use of a blend of PZ, N-methylpiperazine (MPZ), and N,N'-dimethylpiperazine (DMPZ) [3].

Thermal degradation and oxidation are the two primary routes of amine loss during absorption-stripping along with volatilization of the amine in the absorber. Thermal degradation and oxidation of MEA and other alkanolamines have been investigated extensively previously and the impact of degradation was determined to be an important factor in solvent selection [4-12]. The thermal degradation of MEA generated products that have none or only limited CO_2 reactivity, effectively reducing the CO_2 capacity of the solvent. Other classes of amines have been found to generate CO_2-carrying molecules as products that mitigate the overall effect of thermal degradation. For example, concentrated PZ solutions has been found to produce high concentrations of N-formylpiperazine (FPZ), N-(2-aminoethyl)-piperazine (AEP) and ethylenediamine (EDA) during thermal degradation which can react with CO_2 directly (AEP and EDA), or be easily reacted to create PZ (FPZ and other amides) [13]. The same has been seen for N-methyldiethanolamine (MDEA)/PZ which degrades to diethanolamine (DEA) and substituted PZ molecules (1-methylpiperazine, N-(2-hydroxyethyl) piperazine and others) which can react and carry CO_2 during absorption-stripping [14, 15].

The blend of PZ, MPZ and DMPZ offers a solvent that takes advantage of the mixture of multiple amines with CO_2-carrying capacity that can interconvert to become degradation products of each other. The concept is to develop the solvent with a composition stable to thermal degradation that maximizes CO_2 capacity and absorption rate. In developing this solvent, the pertinent physical and thermodynamic properties of the blend that affect its expected performance in a CO_2 capture unit were investigated. Solid solubility, density and viscosity were evaluated over the expected range of CO_2 loading. CO_2 solubility, CO_2 capacity, heat of absorption, amine volatility and CO_2 absorption rate were studied over the pertinent range of lean and rich conditions expected. Finally, the thermal stability and thermal equilibrium of the amine blend were evaluated to determine the degradation potential of the solvent. In each case, the properties of the blend are compared to 8 molal (m) PZ, 7 m MEA, or both solvents to determine the advantages and disadvantages of the solvent compared to current baseline solvents.

1 MATERIALS AND METHODS

1.1 Solution Preparation

Aqueous amine solutions were prepared as described previously with few modifications [13, 16, 17]. Anhydrous PZ (IUPAC: 1,4-diazacyclohexane, CAS 110-85-0, purity 99%, *Acros Organics N.V.*, Geel, Belgium), MPZ (IUPAC: 1-methyl-piperazine, CAS 109-01-3, purity > 99%, *Acros Organics*), and DMPZ (IUPAC: 1,4-dimethyl-piperazine, CAS 106-58-1, purity 98.5%, *Acros Organics*) were obtained commercially and used without further purification. Blends were prepared gravimetrically by combining all three amines with water at the desired concentrations and then heating to melt the PZ. Then, the hot, aqueous solution was transferred to a gas washing bottle where CO_2 (99.5%, *Matheson* Tri Gas, Basking Ridge, NJ, USA) was gravimetrically sparged to achieve the desired CO_2 concentration [16, 17]. Total alkalinity was verified through acid titration and CO_2 concentration was verified through Total Inorganic Carbon (TIC) analysis as described previously [13, 18]. CO_2 loading, α, is reported as mol CO_2/mol alkalinity, which corresponds to mol CO_2/equivalent of amine nitrogen.

1.2 Solid-Liquid Equilibrium Measurements

Solid-liquid equilibrium of blended amine solutions was measured through observation of the conditions under which precipitation occurred. For the amine blend of interest, solutions containing a range of CO_2 loading were prepared by combining unloaded and a maximum rich loaded solution. The maximum rich loaded condition was the highest CO_2 loading found to remain soluble at controlled temperature at or below room temperature. The transition temperature between solid and liquid phases was observed by slowly heating a solution at a given CO_2 loading containing precipitation and observing the phase change, as previously described [16]. All solutions were observed for any precipitation at temperatures between 0°C and the melting point of the solid phase of the amine solution.

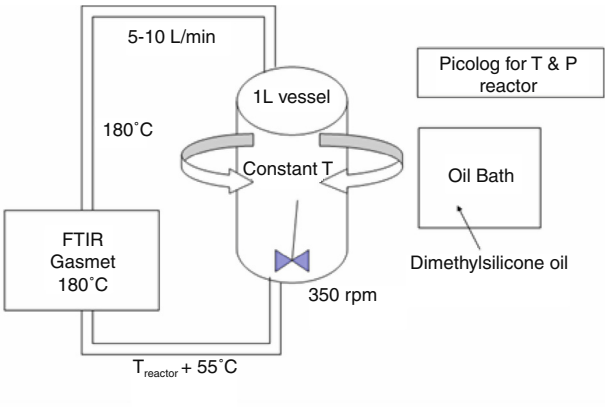

Figure 1

Schematic of equilibrium cell for amine volatility measurement.

1.3 Equilibrium Cell for Volatility

Amine volatility was measured in a stirred 1 L equilibrium cell coupled with a hot gas DX-4000 Fourier Transform Infrared Spectroscopy (FTIR) analyzer (*Gasmet Technologies Inc*., La Prairie, Canada) as shown in Figure 1 and described previously [19]. The insulated glass reactor was agitated at 350 rpm using an overhead stirrer and temperature in the reactor was controlled by recirculating dimethylsilicone oil. Vapor from the headspace of the reactor was pumped at 5 to 10 L/minute through a heated *Teflon*® line to the FTIR. Both the sample line and analyzer were maintained at 180°C to prevent liquid condensation or adsorption of amine. The FTIR quantified amine, CO_2, and water concentration in the vapor phase. After the gas was analyzed in the FTIR, it was returned to the reactor through a second heated line maintained 55°C hotter than the reactor temperature. The 55°C difference was sufficient to ensure that the returned gas did not upset the liquid-vapor equilibrium inside the reactor and to prevent potential heat loss at the bottom of the reactor.

1.4 High Temperature VLE Apparatus for CO_2 Solubility

A high temperature vapor-liquid equilibrium apparatus was used to measure CO_2 solubility in aqueous amine solutions. A 500 mL stainless steel autoclave with an agitator and a heating jacket was used as the equilibrium cell. The method details have been described previously [20]. Total pressure of the CO_2 loaded blend at 100-160°C was measured with ± 2.4 kPa accuracy. CO_2 partial pressure was derived by subtracting partial pressure of N_2 and water from the equilibrium total pressure. Data for the partial pressure of water were taken from the DIPPR database and was assumed to follow Raoult's Law [21]. The partial pressure of nitrogen at the experimental condition was calculated using a low temperature pressure measurement and the assumption that nitrogen behaves as an ideal gas. Liquid samples were collected before and after each experiment at room temperature, analyzed for amine concentration by acid titration and total CO_2 by TIC analysis, and corrected for the gas phase CO_2 at each condition to get CO_2 loading at high temperature.

1.5 Wetted Wall Column for Absorption Rates and CO_2 Solubility

The wetted wall column used in this study to characterize the mass transfer coefficient of amine solution (k'_g) is the same apparatus that had been described previously by Cullinane *et al*. and Dugas *et al*. [22, 23]. In a typical experiment, a gas mixture of nitrogen and CO_2 counter currently contacted the amine solution under study. The flux of CO_2 (N_{CO_2}) between gas and liquid phases for any given condition was calculated from the difference between inlet and outlet CO_2 concentrations quantified using an IR analyzer. By varying the inlet CO_2 partial pressure, both absorption and desorption were observed. The equilibrium CO_2 partial pressure of the amine solution, $P^*_{CO_2,l}$, was calculated using absorption and desorption data to estimate the pressure where zero flux occurs.

The overall mass transfer coefficient (K_G) was calculated as the ratio of the N_{CO_2} and the gas phase partial pressure driving force between the inlet CO_2 partial pressure, $P_{CO_2,g}$ and $P^*_{CO_2,l}$, as shown in Equation (1) :

$$K_G = \frac{N_{CO_2}}{P_{CO_2,\,g} - P^*_{CO_2,1}} \tag{1}$$

The series resistance correlation for gas absorption into liquid is shown in Equation (2). The liquid film mass transfer coefficient based on a partial pressure driving force, k_g', correlates with the experimental conditions and geometry of the apparatus as established above (2):

$$\frac{1}{k'_g} = \frac{1}{K_G} - \frac{1}{k_g} \tag{2}$$

The values for k_g were estimated from a previous correlation [1]. Data for the kinetic absorption rate and CO_2 solubility were obtained simultaneously with this technique.

1.6 Thermal Cylinders for Thermal Degradation

Thermal degradation of amine solutions was assessed using thermal cylinders as described previously [4, 13, 18]. Cylinders consisted of (1/2)-inch OD 316 stainless steel tubing with two stainless steel *Swagelok*® fittings and end caps (*Swagelok Company*, Solon, OH, USA). Cylinders were filled with 10 mL of the amine solution of interest, sealed according to *Swagelok*® specifications, and placed in forced convection ovens maintained at the experimental temperature. Individual cylinders were removed from the oven periodically and the liquid contents were analyzed for total alkalinity and CO_2 concentration, and analyzed using cation ion chromatography to quantify the parent amines and cationic degradation products.

1.7 Cation Ion Chromatography (IC)

Cation Ion Chromatography (cation IC) was used to quantify PZ, MPZ, DMPZ and other cation degradation products in solution. A *Dionex* ICS-2500 Ion Chromatography System with AS autosampler was used as described previously (*Dionex Corporation*, Sunnyvale, CA, USA) [4, 13, 18]. Separation occurred in an IonPac GC17 guard (4 × 50 mm) and CS17 analytical column (4 × 250 mm) with varying concentrations of methanesulfonic acid in analytical grade water and conductivity detector cell.

2 RESULTS AND DISCUSSION

2.1 Physical Properties of PZ/MPZ/DMPZ Blends

2.1.1 Solid Solubility

The solid solubility of 3.75 m PZ/3.75 m MPZ/0.5 m DMPZ with varying concentrations of CO_2 was observed. At room temperature (25°C), a maximum CO_2 loading of 0.39 mol CO_2/mol alkalinity without any solid precipitation was obtained for 3.75 m PZ/3.75 m MPZ/0.5 m DMPZ. At 20°C, a higher maximum loading of 0.43 mol CO_2/mol alkalinity was obtained without solids precipitation. Neither MPZ nor DMPZ were found to precipitate in aqueous solution in the absence of PZ. PZ apparently precipitates as PZ·6H_2O in the blended solvent.

The transition temperature of this blend at 0 to 0.39 mol CO_2/mol alkalinity was observed in order to quantify the solubility envelope where an aqueous amine solution is known to exist. The transition temperature over this range of CO_2 loading for 3.75 m PZ/3.75 m MPZ/0.5 m DMPZ is shown in Figure 2. The transition temperatures of 8 m PZ are included in the figure for comparison purposes [18]. For the blend, the temperature at which any precipitation in the solution completely melted or the liquid precipitated into a solid was obtained and the transition point recorded.

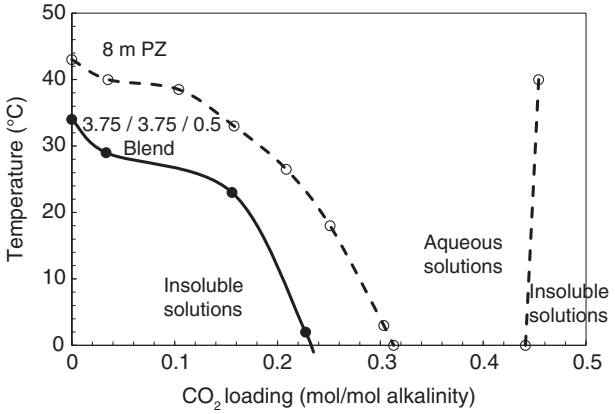

Figure 2

Comparison of solid-liquid transition temperatures of 8 m PZ [18] and 3.75 m PZ/3.75 m MPZ/0.5 m DMPZ.

The blended system has a larger solubility envelope and this solvent is predicted to have fewer solubility issues than a concentrated PZ system. In CO_2-loaded, concentrated PZ, solid PZ hexahydrate (PZ·6H_2O) is formed where the loading is less than 0.22 mol CO_2/mol alkalinity and the temperature is less than 25°C [13]. The blend contains less PZ and PZ·6H_2O, the expected solid formed in the blend in the same region of Figure 2, precipitates at lower temperature and CO_2 loading. This behavior expands the solubility envelope and usefulness of the blend.

At CO_2 loading greater than 0.43 mol CO_2/mol alkalinity, 8 m PZ was found to form hydrated protonated PZ carbamate ($H^+PZCOO^-·H_2O$) when precipitation occurred [16]. No solids precipitated in 3.75 m PZ/3.75 m MPZ/0.5 m DMPZ at any of the high CO_2 concentrations tested. It appears that at least 4 m PZ is required to form significant concentrations of H^+PZCOO^-, so this species is not present to precipitate in its hydrated form in the blended solvent.

2.1.2 Density and Viscosity of 5 M PZ/2 M MPZ/1 M DMPZ

The density and viscosity of 5 m PZ/2 m MPZ/1 m DMPZ were measured from 0 to 0.39 mol CO_2/mol alkalinity and 10 to 80°C (283.15 to 353.15 K). Data were obtained for all solutions where solid precipitation and CO_2 evolution were absent. The raw data are shown

in Table 1 with CO_2 concentration reported in units of CO_2 loading and mol/kg. The density and viscosity data are compared to that of 8 m PZ at 40 and 60°C in Figure 3 and Figure 4, respectively. The data demonstrate the expected trends of increased density and viscosity with increasing CO_2 loading and decreasing temperature. In comparison with 8 m PZ, the blend demonstrates a lower density and higher viscosity at a given CO_2 loading at 40 and 60°C. The higher viscosity of the blend, approximately 25% higher across the board, is a slight disadvantage of this solvent as it is expected to decrease mass transfer and reduce heat transfer coefficients.

The viscosity of 5 m PZ/2 m MPZ/1 m DMPZ is correlated well in terms of the viscosity of water obtained from DIPPR, μ_{water}, CO_2 concentration in mol/kg, C_{CO_2} and temperature in Kelvin, T [21]. The details of the regression and parameters are shown in Equations (3, 4) and Table 2. The regression was able to fit all data

TABLE 1
Density and viscosity of 5 m PZ/2 m MPZ/1 m DMPZ

CO_2 loading (mol/mol alk)	CO_2 (mol/kg)	T (°C)	Density (ρ) (g/cm^3)	Viscosity (μ) (mPa.s)
0.2	1.661	10	1.0937	42.320 ± 0.042
0.23	1.900	10	1.1031	42.940 ± 0.070
0.29	2.411	10	1.1221	44.240 ± 0.070
0.33	2.680	10	1.1358	44.440 ± 0.070
0.37	2.940	10	1.1490	44.390 ± 0.088
0.39	3.105	10	1.1553	44.290 ± 0.120
0.1	0.894	25	1.0553	18.030 ± 0.082
0.15	1.286	25	1.0707	19.290 ± 0.110
0.2	1.661	25	1.0856	20.540 ± 0.178
0.23	1.900	25	1.0955	21.310 ± 0.173
0.29	2.411	25	1.1147	22.790 ± 0.242
0.33	2.680	25	1.1287	23.380 ± 0.199
0.37	2.940	25	1.1421	23.870 ± 0.200
0.39	3.105	25	1.1481	23.960 ± 0.212
0	0	40	1.0117	7.420 ± 0.095
0.05	0.478	40	1.0290	8.261 ± 0.122
0.1	0.894	40	1.0457	9.154 ± 0.148
0.15	1.286	40	1.0618	9.993 ± 0.157
0.2	1.661	40	1.0772	10.900 ± 0.226
0.23	1.900	40	1.0874	11.390 ± 0.213
0.29	2.411	40	1.1073	12.570 ± 0.206
0.33	2.680	40	1.1214	13.290 ± 0.311
0.37	2.940	40	1.1347	13.680 ± 0.319
0.39	3.105	40	1.1408	13.960 ± 0.337
0	0	60	0.9957	3.666 ± 0.125

(continued)

TABLE 1 *(continued)*

CO_2 loading (mol/mol alk)	CO_2 (mol/kg)	T (°C)	Density (ρ) (g/cm^3)	Viscosity (μ) (mPa.s)
0.05	0.478	60	1.0139	4.157 ± 0.124
0.1	0.894	60	1.0317	4.698 ± 0.180
0.15	1.286	60	1.0486	5.310 ± 0.226
0.2	1.661	60	1.0644	5.900 ± 0.243
0.23	1.900	60	1.0750	6.354 ± 0.246
0.29	2.411	60	1.0951	7.045 ± 0.293
0.33	2.680	60	1.1097	7.698 ± 0.369
0	0	80	0.9786	2.035 ± 0.051
0.05	0.478	80	0.9978	2.289 ± 0.104
0.1	0.894	80	1.0165	2.628 ± 0.123
0.15	1.286	80	1.0337	3.039 ± 0.142
0.20	1.661	80	1.0511	3.277 ± 0.160
0.23	1.900	80	1.0614	3.696 ± 0.103
0.29	2.411	80	-	4.163 ± 0.192
0.33	2.680	80	-	5.350 ± 0.196

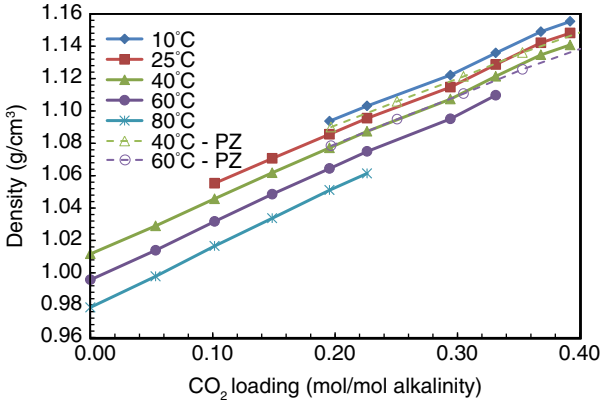

Figure 3

A comparison of the density of 5 m PZ/2 m MPZ/1 m DMPZ at 10 (◆), 25 (■), 40 (▲), 60 (●), and 80°C (*) and 8 m PZ at 40 (Δ) and 60°C (○).

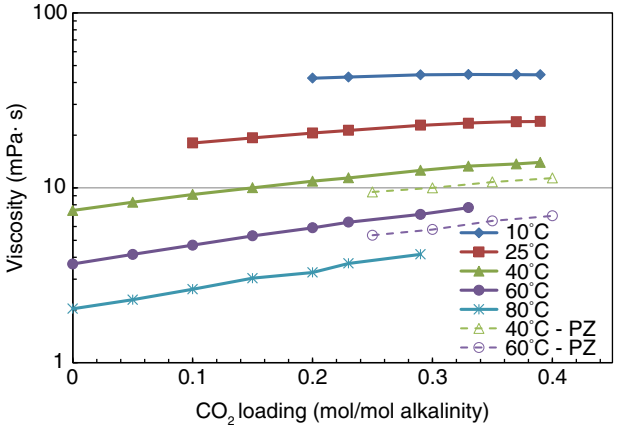

Figure 4

A comparison of the viscosity of 5 m PZ/2 m MPZ/1 m DMPZ at 10 (◆), 25 (■), 40 (▲), 60 (●), and 80 °C (*) and 8 m PZ at 40 (Δ) and 60°C (○).

with an average error of only 2.0% and a maximum deviation of 5.1%:

$$\ln\left(\frac{\mu}{\mu_{water}}\right) = \phi_1 + \phi_2 \cdot T + \frac{\phi_3}{T} \quad (3)$$

$$\phi_i = a_i + b_i \times C_{CO_2} \quad (4)$$

2.2 Thermodynamic Properties of PZ/MPZ/DMPZ

2.2.1 CO_2 Solubility

The CO_2 partial pressure, P_{CO_2}, of 3.75 m PZ/3.75 m MPZ/0.5 m DMPZ was measured from 40 to 160°C for a range of CO_2 loading. Data were obtained from the

TABLE 2
Value of parameters in Equation (4)

Parameter	$i = 1$	$i = 2$	$i = 3$
a	−29.12	0.0379	6 167.9
b	6.151	−0.00746	−1 131.04

equilibrium cell at 40°C, the wetted wall column for 40 to 100°C, and the high temperature VLE apparatus from 100 to 160°C. The total pressure, P_{total}, was obtained from the high temperature measurements and the P_{CO_2} was estimated as described above. The CO_2 solubility values measured directly from the equilibrium cell and wetted wall column are compared in Table 3. The estimated P_{CO_2} and P_{total} measurements are shown in Table 4.

The CO_2 solubility measured from 40 to 160°C is shown in Figure 5 as the P_{CO_2} plotted against the CO_2 loading. Data from three separate experimental apparatuses, the wetted wall column, high temperature VLE apparatus and equilibrium cell, are shown and demonstrate strong agreement that provides confidence in the data. An empirical model for the prediction of P_{CO_2} was developed using the data from 40 to 160°C (excluding the single point from the equilibrium cell). The regressed form of the model is shown in Equation (5) where the natural log of P_{CO_2} in Pa is predicted as a function of CO_2 loading, α, and temperature in K, T. The uncertainty of the regression is demonstrated by the error for each of the three regressed coefficients:

$$\ln P_{CO_2} = (34.4 \pm 0.2) + \frac{(-10597 \pm 81)}{T} + (7627 \pm 177) \cdot \frac{\alpha}{T} \quad (5)$$

2.2.2 CO_2 Capacity

The intrinsic CO_2 capacity of 3.75 m PZ/3.75 m MPZ/0.5 m DMPZ was estimated assuming lean loading (0.23 mol CO_2/mol alkalinity) and rich loading (0.33 mol CO_2/mol alkalinity) that correspond to P_{CO_2} values at 40°C of 0.5 and 5 kPa, respectively. These two pressure values are estimates of the P_{CO_2} that would provide an appropriate driving force at the bottom or top of the absorber [1, 24]. With the appropriate unit conversions, the capacity of the blend is 0.88 mol CO_2/kg (amine + water). This compares to an intrinsic CO_2 capacity of 0.79 and 0.47 mol CO_2/kg (amine + water) for 8 m PZ and 7 m MEA, respectively [25, 26].

2.2.3 Estimation of Heat of Absorption

The heat of CO_2 absorption (ΔH_{abs}) in 3.75 m PZ/3.75 m MPZ/0.5 m DMPZ was estimated from the derivative of Equation (5) according to the Gibbs-Helmholtz Equation (*Eq. 6*) and is given by Equation (7). Over the expected CO_2 loading range, 0.23 to 0.33 mol CO_2/mol

TABLE 3
CO_2 partial pressure and mass transfer coefficient for 3.75 m PZ/3.75 m MPZ/0.5 m DMPZ

T (°C)	CO_2 loading (mol/mol alk)	P_{CO_2} (kPa)	k'_g (mol/s.Pa.m^2)	Source(1)
40	0.21	0.3	2.5×10^{-6}	WWC
40	0.23	0.3	–	EC
40	0.25	0.8	1.2×10^{-6}	WWC
40	0.29	2.1	9.2×10^{-7}	WWC
40	0.32	4.5	5.6×10^{-7}	WWC
60	0.21	1.7	2.6×10^{-6}	WWC
60	0.25	3.8	1.5×10^{-6}	WWC
60	0.29	9.9	8.7×10^{-7}	WWC
60	0.32	19.0	5.1×10^{-7}	WWC
80	0.21	8.0	2.1×10^{-6}	WWC
80	0.25	16.8	1.1×10^{-6}	WWC
100	0.21	29.2	1.3×10^{-6}	WWC

(1) WWC = wetted wall column; EC = equilibrium cell.

TABLE 4
Total pressure and estimated P_{CO_2} of 3.75 m PZ/3.75 m MPZ/0.5 m DMPZ from high temperature VLE apparatus

T (°C)	CO_2 loading (mol/mol alk)	P_{total} (kPa)	Estimated P_{CO_2} (kPa)
100	0.24	129	40.8
100	0.32	360	271
110	0.32	573	447
120	0.24	334	160
120	0.31	865	690
130	0.24	506	270
130	0.30	1 257	1 020
140	0.23	771	456
140	0.29	1 790	1 470
150	0.23	1 142	730
150	0.28	2 437	2 020
160	0.22	1 647	1 110
160	0.27	3 269	2 730

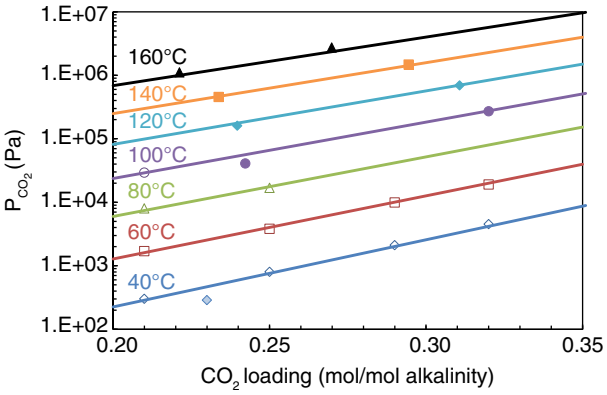

Figure 5

Solubility of CO_2 in 3.75 m PZ/3.75 m MPZ/0.5 m DMPZ from 40 to 160°C. Data: wetted wall column (open points), high temperature VLE apparatus (closed points), equilibrium cell (shaded point); lines: Equation (5).

alkalinity, the ΔH_{abs} predicted with Equation (7) varies from 73.5 to 67.2 kJ/mol:

$$\Delta H_{abs} = -R\frac{\partial(\ln P_{CO_2})}{\partial\left(\frac{1}{T}\right)} \quad (6)$$

$$\Delta H_{abs} = -R \cdot (-10597 + 7627 \cdot \alpha) \quad (7)$$

2.2.4 Amine Volatility

The volatility of amines in 3.75 m PZ/3.75 m MPZ/0.5 m DMPZ was measured at 40°C and a nominal lean loading of 0.23 mol CO_2/mol alkalinity, the conditions expected at the top of the absorber. The conditions that exist at the top of the absorber are the most important for volatility comparisons in order to assess potential fugitive losses to the atmosphere. For this solvent, this condition resulted in a P_{CO_2} of 287 Pa and partial pressure of water, P_{H_2O}, or 5 875 Pa. The measured amine volatility of each of the three amine components in the blend is presented in Table 5 as the partial pressure of each amine (P_{PZ}, P_{MPZ} and P_{DMPZ}). The amine volatility for 8 m PZ and 7 m MEA are also shown for comparison purposes [19]. The CO_2 loading for these two baseline systems were also chosen to mimic the operating conditions expected at the top of the absorber.

Based on the results, it is clear that methylation increases volatility. The volatility of MPZ and DMPZ are significantly higher than that of PZ in the blend and by itself, suggesting a significant impact of methylation on the behavior of the amino function. Even though DMPZ is present only in a small concentration, 0.5 m, its volatility is the highest and 65 times greater than PZ. The fact that this molecule has two methyl groups renders it fairly nonpolar in the polar environment consisting of water and electrolytes. Therefore, DMPZ has

TABLE 5
Amine volatility for 3.75 m PZ/3.75 m MPZ/0.5 m DMPZ, 8 m PZ and 7 m MEA at 40°C

Solvent	3.75 m PZ/3.75 m MPZ/ 0.5 m DMPZ	8 m PZ	7 m MEA
CO_2 loading (mol/mol alk)	0.23	0.29	0.47
P_{PZ} (Pa)	0.95	0.8	-
P_{MPZ} (Pa)	16.4	-	-
P_{DMPZ} (Pa)	64.1	-	-
P_{MEA} (Pa)	-	-	2.7

unfavorable interactions with the surrounding species and is highly volatile. MPZ also suffers the effects of a nonpolar methyl group but to a lesser extent than DMPZ. This observation highlights the fact that degradation products can be more volatile than the parent amine itself, even at small concentrations, an important fact in solvent selection.

2.2.5 CO_2 Absorption Rate

The liquid film mass transfer coefficient (k_g') for 3.75 m PZ/3.75 m MPZ/0.5 m DMPZ was measured from 40 to 100°C at a range of loadings (*Fig. 6* and *Tab. 3*). The use of P_{CO_2} at 40°C as the abscissa allows direct comparison of rate data at different temperature as well as for different amine solvents on the same basis without influences from differences in CO_2 loading. The range of P_{CO_2} from 0.5 to 5 kPa, as used previously for capacity calculations, represents a reasonable driving force between gas and liquid at the top and bottom of an absorber expected during the treatment of flue gas from coal-fired power plant. At 0.5 kPa and 40°C, the expected conditions at the lean end of the absorber, the kg' of the blend is 2.0×10^{-6} mol/s.Pa.m^2 compared to 2.1×10^{-6} and 7.6×10^{-7} mol/s.Pa.m^2 for PZ and MEA, respectively.

The temperature range expected for the absorber is 40 to 60°C. In this temperature range, the rate for the blend stays relatively constant, approximately equal to that for 8 m PZ and over 2.5 times faster than 7 m MEA. Temperature above 60°C leads to a decrease in the mass transfer rate of the blend, as has been observed for other amine systems [24-26]. The blend performed as well as concentrated PZ and represents another solvent that can outperform the baseline MEA solvent.

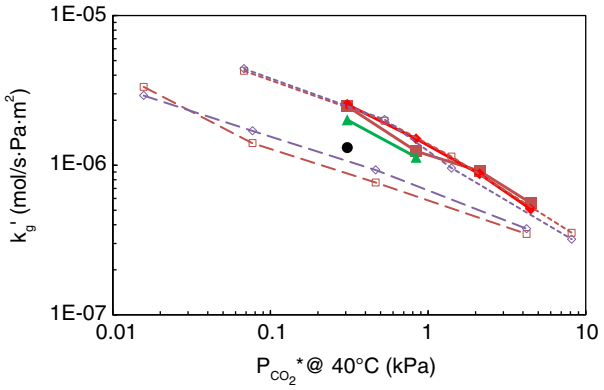

Figure 6

Mass transfer coefficient of 3.75 m PZ/3.75 m MPZ/0.5 m DMPZ (solid points) at temperatures 40 (■), 60 (◆), 80 (▲), and 100°C (●), compared with 8 m PZ (short dash with open points) and 7 m MEA (long dash with open points) at 40 and 60°C.

2.3 Behavior of the Blend at High Temperature

2.3.1 Thermal Degradation of the PZ-Based Blends

The thermal behavior of PZ/MPZ/DMPZ was studied at 150°C. This temperature represents the expected temperature of the stripper and reboiler section of an absorber-stripper system utilizing a thermally stable solvent in order to maximize high temperature energy savings.

Six PZ-based solvent blends were investigated for their thermal stability. All blends are compared to 8 m PZ as the baseline case of a highly stable solvent. In the blends tested, the total alkalinity of the solvent was maintained at 8 m, while PZ was replaced with methylated PZ molecules (MPZ or DMPZ). Blend compositions are indicated as the concentration of PZ/MPZ/DMPZ, all in units of m. For example, one two-component blend of 4 m PZ/4 m MPZ, or 4/4/0, was investigated. Five three-component blends (5/2/1, 5/2.5/0.5, 5/1.5/1.5, 3.9/3.9/0.2, and 3.75/3.75/0.5) were also investigated.

The overall rate of thermal degradation was assessed using a first order rate constant of amine loss, k_1, as described in detail previously [13, 27]. For comparing the blends, the rate was determined based on the total amine loss as a sum of PZ, MPZ and DMPZ rather than the rate of loss of the individual amine species. This was done to allow an overall comparison of the blends on a similar basis. The k_1 values for thermal degradation at 150°C of the 8 m PZ and the blends are compared in Table 6. The k_1 values of the blends vary from 8.6×10^{-9} to 7.5×10^{-8} s^{-1} and are substantially less than the comparable value for 7 m MEA with 0.4 mol CO_2/mol alkalinity degraded at 150°C of 8.3×10^{-7} s^{-1} [4].

Blending of PZ with MPZ and DMPZ also reduces solvent stability as shown with the high k_1 values for all blends studied. The changes in the rate constant are small for most of the blends with the exception of the 5/1.5/1.5 solvent, so the slight increase in degradation may be balanced by the improvement in solid solubility.

2.3.2 Thermal Equilibrium of PZ, MPZ and DMPZ

A thermal equilibrium was found to establish itself in the presence of methylated PZ. In the degradation of 8 m MPZ, PZ and DMPZ were generated as products through a S_N2-type substitution or arm-switching reaction. Observations of this system indicate it tends toward an equilibrium set of concentrations as the species interconvert to produce a solvent that is thermally stable at its equilibrium concentrations. The thermal equilibrium established between PZ, MPZ, and DMPZ was studied in the thermal degradation experiments performed at 150°C described in the previous section. At this temperature, some degradation was expected to occur, but the interconversion of PZ, MPZ and DMPZ was assumed to occur more rapidly than degradation processes based on the slow degradation rates discussed in the previous section.

TABLE 6

First-order rate constant for amine thermal degradation at 150°C with 0.3 mol CO_2/mol alkalinity calculated based on total amine loss

PZ/MPZ/DMPZ concentration (m)	$k_1 \times 10^{-9}$ at 150°C (s^{-1})
0/8/0	8.6
3.75/3.75/0.5	10.3
3.9/3.9/0.2	8.4
4/4/0	13.9
5/1.5/1.5	75.3
5/2/1	13.7
5/2.5/0.5	14.4
8 m PZ	6.1
7 m MEA	828

The expected equilibrium reaction of MPZ is as follows, where the brackets indicate the concentration of the given species in units of mmol/kg (*Eq. 8*). The equilibrium constant, K_{eq}, of Equation (8) can then be calculated (*Eq. 9*):

$$2[\mathrm{MPZ}] \leftrightarrow [\mathrm{PZ}] + [\mathrm{DMPZ}] \quad (8)$$

$$K_{eq} = \frac{[\mathrm{PZ}]\,[\mathrm{DMPZ}]}{[\mathrm{MPZ}]^2} \quad (9)$$

The goal of this K_{eq} analysis is to determine the concentrations of the three amine species in equilibrium at 150°C. These concentrations would be what were expected to be stable in a system with a reboiler temperature of 150°C. The K_{eq} values for the thermal equilibrium of PZ, MPZ, and DMPZ are shown in Figure 7. For each blend, the K_{eq} was calculated at each time point according to Equation (9) and plotted against degradation time.

All of the experiments, including those with limited data, were found to tend toward a K_{eq} value of 0.27-0.30, indicating the equilibrium concentrations of amine expected at 150°C. The experiments containing 3.9/3.9/0.2 and 3.75/3.75/0.5 demonstrate this tendency toward a K_{eq} of 0.29. Experiments with initial amine concentrations far from equilibrium, such as the 5/1.5/1.5 blend, demonstrated a higher thermal degradation rate as the amines reacted toward equilibrium, as shown in Table 6.

Degradation of PZ alone will not yield these results as MPZ and DMPZ are only minor products [13]. However, when a blend begins with at least some N-methylated PZ (*i.e.*, MPZ or DMPZ), these methyl groups can easily

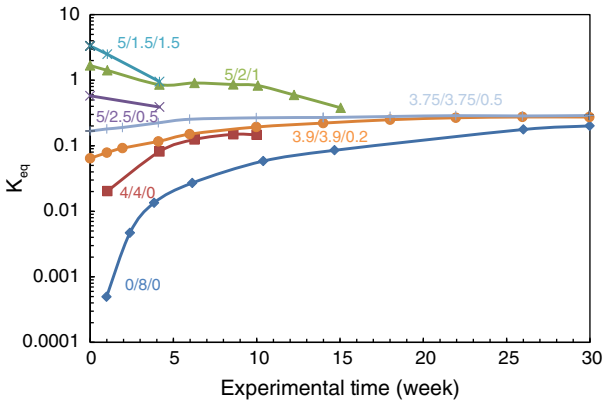

Figure 7

K_{eq} for PZ + MPZ + DMPZ solutions thermally degraded at 150°C ($\alpha = 0.3$). Labels indicate the concentrations of PZ, MPZ, and DMPZ in solution in molal (m).

TABLE 7
Comparison of CO_2 capture solvents

Solvent	7 m MEA	8 m PZ	3.75 m PZ/3.75 m MPZ/ 0.5 m DMPZ
Solubility range at 20°C (mol CO_2/mol alkalinity)	0 to max	0.25-0.45	0.18 to max
Operating loading range (mol CO_2/mol alkalinity)	0.45-0.55	0.31-0.39	0.23-0.32
CO_2 capacity (mol/kg amine + water)	0.47	0.79	0.88
k_g'$_{avg}$ (40°C) (mol/s.Pa.m^2)	4.3×10^{-7}	8.5×10^{-7}	8.5×10^{-7}
ΔH_{abs} (kJ/mol CO_2)	72 ± 4	66 ± 2	70 ± 1
P_{amine} at lean ldg and 40°C (Pa)	2.7	0.8	81.5
Thermal degradation, $k_1 \times 10^{-9}$ at 150°C (s^{-1})	828	6.1	10.3

undergo a straightforward nucleophilic attack and disproportionation, resulting in switching of the methyl groups between molecules. Overall, the data suggest that any system starting with MPZ will tend toward a K_{eq} of 0.28 to 0.30 at 150°C.

2.4 Overall Comparison of Blends

A comparison of the important parameters for CO_2 capture solvents is presented in Table 7 for 7 m MEA, 8 m PZ, and 3.75 m PZ/3.75 m MPZ/0.5 m DMPZ. The CO_2 loading range when the solvent is completely soluble at 20°C is shown based on solubility data. The improved solubility of both MEA and the blend is a strong advantage over 8 m PZ. The CO_2 capacity was calculated for each system as described in Section 2.2.2 based on CO_2 solubility at P_{CO_2} of 0.5 and 5 kPa. The blend and 8 m PZ have approximately double the CO_2 capacity as MEA, an important advantage. The average k'_g, $k'_{g\ avg}$, based on a log-mean flux and log-mean driving force across a typical absorber design, as described in detail previously, is compared at 40°C [26]. Both PZ and the blend have k_g'$_{avg}$ values double that of MEA.

Empirical regressions for the ΔH_{abs} are shown for each solvent based on CO_2 solubility regressions developed for MEA and PZ previously or for the blend as described in this manuscript [20]. The ΔH_{abs} was calculated from the empirical regressions at a midpoint in the expected loading range for each amine system. The midpoint was determined to be at a P_{CO_2} of 1.5 kPa, which corresponded to CO_2 loadings of 0.49, 0.35, and 0.28 mol CO_2/mol alkalinity for the MEA, PZ and blended systems, respectively. Error in the calculation of this value was assessed based on the confidence of each regressed coefficient. The larger ΔH_{abs} for the blend over PZ is a crucial advantage that will reduce overall energy performance.

Volatility was reported as the overall amine volatility of each solvent at 40°C at the expected lean loading as this should correspond to the top of the absorber in a real system. For the blend, this is a sum of the partial pressure of PZ, MPZ and DMPZ at this condition. The volatility of the blend is significantly higher than the two baseline amines. Implementation of this amine system will require an adequately designed water wash system to avoid amine losses from the absorber.

The thermal stability of each solvent is expressed as the k_1 for thermal degradation at 150°C. Data for MEA, PZ and the blend were obtained at 0.4, 0.3 and 0.3 mol CO_2/mol alkalinity, respectively. The reported value for the blend is based on total amine loss from PZ, MPZ and DMPZ. Both PZ and the blend are significantly more thermally stable than MEA as demonstrated by the large k_1 value of MEA.

CONCLUSIONS

A blend of PZ, MPZ and DMPZ is an example of a new solvent design based on the thermal equilibrium of multiple amines useful for CO_2 capture. Blends of this nature reach a thermal equilibrium at reboiler temperature where the overall thermal degradation rate is low while multiple species exist that are valuable to the CO_2 capture process. 3.75 m PZ/3.75 m MPZ/0.5 m DMPZ has been fully evaluated for this application.

In comparison with 8 m PZ, this blend was found to have advantageous solid solubility and ΔH_{abs}, with approximately the same behavior in terms of CO_2

capacity, CO_2 absorption rate and thermal degradation as shown in Table 7. Disadvantages of the blend include mildly increased viscosity and substantially greater amine volatility as DMPZ. Both of these properties are important to the optimized design of a CO_2 capture system and would need to be addressed. A carefully designed water wash system would be needed to address the amine volatility. As with PZ, the blend was found to have significantly better CO_2 capacity, CO_2 absorption rates and thermal stability compared to 7 m MEA.

ACKNOWLEDGMENTS

The Luminant Carbon Management Program provided support for this work.

REFERENCES

1 Dugas R.E. (2009) Carbon Dioxide Absorption, Desorption, and Diffusion in Aqueous Piperazine and Monoethanolamine, *PhD Thesis*, The University of Texas, Austin.

2 Rochelle G.T., Chen E., Freeman S.A., Van Wagener D.H., Xu Q., Voice A.K. (2011) Aqueous piperazine as the new standard for CO_2 capture technology, *Chem. Eng. J.* **171**, 3, 725-733.

3 Rochelle G.T., Freeman S.A., Chen Xi, Nguyen Thu, Voice A., Rafique H. Acidic gas removal by aqueous amine solvents, U.S. Patent Application 2011/0171093 (PCT Patent Application W02011088008).

4 Davis J.D. (2009) Thermal Degradation of Aqueous Amines Used for Carbon Dioxide Capture, *PhD Thesis*, The University of Texas, Austin.

5 Davis J.D., Rochelle G.T. (2009) Thermal degradation of monoethanolamine at stripper conditions, *Energy Procedia* **1**, 327-333.

6 Meisen A., Kennard M.L. (1982) DEA degradation mechanism, *Hydrocarbon Process.* **61**, 105-108.

7 Rochelle G.T. (2009) Amine Scrubbing for CO_2 Capture, *Science* **325**, 1652-1654.

8 Sexton A.J. (2008) Amine Oxidation in CO_2 Capture Processes, *PhD Thesis*, The University of Texas, Austin.

9 Sexton A.J., Rochelle G.T. (2011) Reaction Products from the Oxidative Degradation of Monoethanolamine, *Ind. Eng. Chem. Res.* **50**, 1, 667-673.

10 Strazisar B.R., Anderson R.R., White C.M. (2003) Degradation Pathways for Monoethanolamine in a CO_2 Capture Facility, *Energy Fuels* **17**, 4, 1034-1039.

11 Chakma A., Meisen A. (1987) Degradation of aqueous DEA solutions in a heat transfer tube, *Can. J. Chem. Eng.* **65**, 2, 264-273.

12 Chakma A., Meisen A. (1997) Methyl-diethanolamine degradation - Mechanism and kinetics, *Can. J. Chem. Eng.* **75**, 5, 861-871.

13 Freeman S.A. (2011) Thermal Degradation and Oxidation of Aqueous Piperazine for Carbon Dioxide Capture, *PhD Thesis*, The University of Texas, Austin.

14 Closmann F., Nguyen T., Rochelle G.T. (2009) MDEA/Piperazine as a solvent for CO_2 capture, *Energy Procedia* **1**, 1351-1357.

15 Closmann F., Rochelle G.T. (2011) Degradation of aqueous methyldiethanolamine by temperature and oxygen cycling, *Energy Procedia* **4**, 23-28.

16 Freeman S.A., Dugas R.E., Van Wagener D.H., Nguyen T., Rochelle G.T. (2010) Carbon dioxide capture with concentrated, aqueous piperazine, *Int. J. Greenhouse Gas Control* **4**, 2, 119-124.

17 Hilliard M.D. (2008) A Predictive Thermodynamic Model for an Aqueous Blend of Potassium Carbonate, Piperazine, and Monoethanolamine for Carbon Dioxide Capture from Flue Gas, *PhD Thesis*, The University of Texas, Austin.

18 Freeman S.A., Davis J.D., Rochelle G.T. (2010) Degradation of aqueous piperazine in carbon dioxide capture, *Int. J. Greenhouse Gas Control* **4**, 5, 756-761.

19 Nguyen T., Hilliard M.D., Rochelle G.T. (2010) Amine volatility in CO_2 capture, *Int J. Greenhouse Gas Control* **4**, 5, 707-715.

20 Xu Q., Rochelle G.T. (2011) Pressure and CO_2 Solubility at High Temperature in Aqueous Amines, *Energy Procedia* **4**, 117-124.

21 DIPPR (2010) *DIPPR 801 Database of Physical and Thermodynamic Properties of Pure Chemicals*, Brigham Young University.

22 Cullinane J.T., Rochelle G.T. (2006) Kinetics of carbon dioxide absorption into aqueous potassium carbonate and piperazine, *Ind. Eng. Chem. Res.* **45**, 8, 2531-2545.

23 Dugas R.E., Rochelle G.T. (2009) Absorption and desorption rates of carbon dioxide with monoethanolamine and piperazine, *Energy Procedia* **1**, 1163-1169.

24 Dugas R.E., Rochelle G.T. (2011) CO_2 Absorption Rate into Concentrated Aqueous Monoethanolamine and Piperazine, *J. Chem. Eng. Data* **56**, 2187-2195.

25 Chen X., Closmann F., Rochelle G.T. (2011) Accurate screening of amines by the Wetted Wall Column, *Energy Procedia* **4**, 101-108.

26 Chen X., Rochelle G.T. (2011) Aqueous Piperazine Derivatives for CO_2 Capture: Accurate Screening by a Wetted Wall Column, *Chem. Eng. Res. Des.* **89**, 9, 1693-1710.

27 Freeman S.A., Rochelle G.T. (2011) Thermal degradation of piperazine and its structural analogs, *Energy Procedia* **4**, 43-50.

Manuscript accepted in November 2012
Published online in August 2013